

SERI/TP-35-253  
UC CATEGORY: UC-64

ANALYSIS OF A HEAT EXCHANGER-  
THERMOELECTRIC GENERATOR SYSTEM

JON HENDERSON

TO BE PRESENTED AT THE 14TH  
INTERSOCIETY ENERGY CONVERSION  
ENGINEERING CONFERENCE

BOSTON, MASSACHUSETTS

AUGUST 5-10, 1979

**Solar Energy Research Institute**

1536 Cole Boulevard  
Golden, Colorado 80401

A Division of Midwest Research Institute

Prepared for the  
U.S. Department of Energy  
Contract No. EG-77-C-01-4042

ANALYSIS OF A HEAT EXCHANGER-THERMOELECTRIC GENERATOR SYSTEM

Jon Henderson  
Solar Energy Research Institute  
Golden, Colorado 80401  
A Division of Midwest Research Institute

ABSTRACT

Analysis of a thermoelectric generator (TEG) in an ocean thermal energy conversion (OTEC) application is presented. An analytic model is developed for describing the heat exchanger-TEG interactions. This model is used to illustrate limitations of applying conventional fixed junction temperature assumptions to systems experiencing significant temperature drops across the heat exchanger surfaces. Design methods are developed for determining the thermoelectric element geometry that produces maximum output power. Results show that a heat exchanger-TEG system may deliver about  $100 \text{ W/m}^2$  of heat exchanger surface. This compares favorably with conventional OTEC schemes.

RECENT WORK performed at the Solar Energy Research Institute has considered thermoelectric generators (TEGs) for electric power generation from low temperature solar thermal sources, such as ocean thermal layers or salinity gradient ponds (1\*). These applications consider a TEG sandwiched between the warm and cold flow channels of a plate-fin or parallel-plane heat exchanger. Mathematical analysis of TEG systems is relatively straightforward; however, no previous investigations addressing this type of heat exchanger-TEG system were uncovered by the author. Most conventional design methods assume known, fixed temperatures at the warm and cold junctions. This approach fails to address the temperature dependence between the energy flux passing through the TEG and the associated temperature drops across the heat exchanger surfaces. Since these temperature drops strongly affect power generation and are sensitive to TEG design, fixed temperature techniques are inadequate for this analysis. Fixed heat input TEG analysis considers variations in junction temperatures but is intended for systems significantly different from ocean thermal energy conversion (OTEC) or other fixed-temperature-source applications.

This paper describes an analytic model suitable for predicting performance of a heat exchanger-TEG system. The model is used to illustrate the limitation of applying conventional fixed junction temperature analysis when significant temperature drops occur across the heat exchanger surfaces. An OTEC performance analysis is included that shows the relationship between the ratio of thermoelectric element area to length and the output power generated by a TEG using standard maximum efficiency and maximum power fixed junction temperature design constraints.

For OTEC applications, the thermal energy source is free. Thus, the cost of power is controlled by the cost of the conversion equipment. The cost of electrical energy for a given heat exchanger is minimized

by maximizing the TEG power generation. The method of Lagrange multipliers is used to solve numerically the heat exchanger-TEG model for the maximum power generation condition. This technique is rather tedious; therefore, a simplified approximate technique to design a TEG that delivers maximum power within a heat exchanger-TEG system is also developed.

NOMENCLATURE

A,B,C,D,E,F	heat exchanger-TEG constants defined in text
COV	fraction of heat exchanger surface covered with thermoelectric material
$h_c$	heat transfer coefficient between cold flow and TEG cold junction
$h_w$	heat transfer coefficient between warm flow and TEG warm junction
I	current
K	conduction heat transfer coefficient through the TEG
$L_1, L_2, L_3$	Lagrange multipliers
m	$Y_n/Y_p$
n	$R_l/R$
P	TEG electrical power output
$q_w, q_c$	heat fluxes at the TEG warm and cold junctions
R	internal resistance of TEG
$R_l$	electric load resistance
$R_t$	total circuit resistance
$T_{wj}$	TEG warm junction temperature
$T_{cj}$	TEG cold junction temperature
$\Delta T_c$	temperature difference between the TEG cold junction and the cold flow
$\Delta T_{teg}$	temperature difference across the TEG junctions
$\Delta T_w$	temperature difference between the warm flow and the warm TEG junction
Z	$\Delta T_{teg}/R_t$
$\alpha$	Seebeck coefficient of the TEG
$\alpha_n, \alpha_p$	Seebeck coefficients of the n-type and p-type thermoelectric materials
$\gamma$	$\gamma_p \times COV$
$Y_n, Y_p$	ratios of the thermoelectric element area to length for the n-type and p-type materials
$\eta$	TEG conversion efficiency
$\lambda_n, \lambda_p$	thermal conductivities of the n and p thermoelectric materials
$\rho_n, \rho_p$	resistivities of the n and p thermoelectric materials
$\nabla$	gradient operator

HEAT EXCHANGER-TEG DISCUSSION

A typical thermoelectric element configuration is assumed and illustrated in Fig. 1. The analysis is developed by incorporating thermoelectric theory with the heat transfer coefficients of the heat exchanger. Assumptions used in this paper are:

- The heat exchanger heat transfer coefficients include the thermal resistance of the TEG electrical insulation in addition to the thermal resistances

\*Numbers in brackets designate References at end of paper.

associated with the flow boundary layer and the heat exchanger material.

- The thermal resistance between thermoelectric materials is assumed to introduce negligible conduction losses.
- Contact electric resistance is insignificant relative to the electric resistance of the thermoelectric elements.
- The analysis is performed on a single thermoelectric element. Power is investigated, but output voltage and current remain dependent on the connection scheme.
- The device operates under small temperature differences so that thermoelectric material properties remain constant. Thus, Thomson effects are neglected.

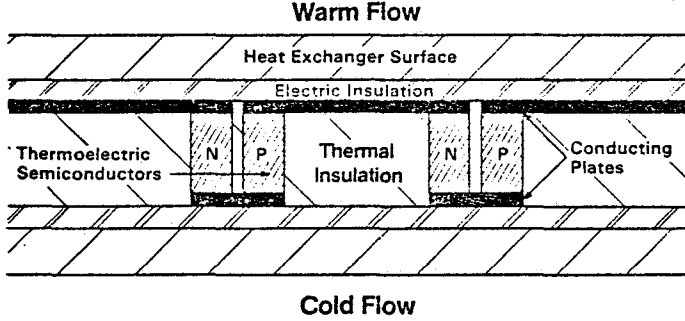


Fig. 1 - Thermocouple detail

The generator performance is determined by equating the heat fluxes across the heat exchanger surfaces to the heat fluxes at the warm and cold junctions of the thermoelectric generator.

$$q_w = \Delta T_w h_w \quad (1)$$

$$q_w = K \Delta T_{teg} + \alpha I T_{wj} - \frac{1}{2} I^2 R \quad (2)$$

$$q_c = \Delta T_c h_c \quad (3)$$

$$q_c = K \Delta T_{teg} + \alpha I T_{cj} + \frac{1}{2} I^2 R \quad (4)$$

The heat fluxes through the warm and cold sides of the heat exchanger are determined from the associated thermal conduction coefficients. The heat fluxes at the thermoelectric junctions are slightly more complicated. At these junctions the heat flux is due to the sum of thermal conduction, the Peltier effect, and joule heating (2). The joule heating within the generator is assumed to disperse evenly between the warm and cold junctions.

The lumped-parameters used to describe the thermal and electrical properties of the generator are determined from:

$$K = (\gamma_n \lambda_n + \gamma_p \lambda_p) COV \quad (5)$$

$$\alpha = |\alpha_n| + |\alpha_p| \quad (6)$$

$$R = \frac{\rho_n / \gamma_n + \rho_p / \gamma_p}{COV} \quad (7)$$

By using the relationships between the temperatures:

$$T_{wj} = T_w - \Delta T_w \quad (8)$$

$$T_{cj} = T_w - \Delta T_w - \Delta T_{teg} \quad (9)$$

$$\Delta T_c = T_w - \Delta T_w - \Delta T_{teg} - T_c \quad (10)$$

and the following expressions for the total resistance and TEG current:

$$R_t = R + R_l \quad (11)$$

$$I = \frac{\alpha \Delta T_{teg}}{R_t} \quad (12)$$

Eqs. (1) through (4) can be solved for  $\Delta T_w$ . Eqs. (1) and (2) yield

$$\Delta T_w = \frac{2R_t^2 K \Delta T_{teg} + 2R_t \alpha^2 T_w \Delta T_{teg} - R \alpha^2 \Delta T_{teg}^2}{2R_t^2 h_w + 2R_t \alpha^2 \Delta T_{teg}} \quad (13)$$

and Eqs. (3) and (4) produce the expression

$$\begin{aligned} \Delta T_w = & [2R_t^2 h_c (T_c - T_w) + 2R_t^2 (h_c + K) \Delta T_{teg} + 2R_t \alpha^2 T_w \Delta T_{teg} \\ & + 2R_t \alpha^2 \Delta T_{teg}^2 + R \alpha^2 \Delta T_{teg}^2] \\ & \times (2R_t \alpha^2 \Delta T_{teg} - 2R_t^2 h_c)^{-1} \quad (14) \end{aligned}$$

By equating these two expressions and performing algebraic manipulation, a third-order polynomial in  $\Delta T_{teg}/R_t$  results:

$$\begin{aligned} AR_t \left( \frac{\Delta T_{teg}}{R_t} \right)^3 + B(2R_t + R) \left( \frac{\Delta T_{teg}}{R_t} \right)^2 \\ + [2R_t (h_w h_c + h_w K + h_c K) + C] \left( \frac{\Delta T_{teg}}{R_t} \right) + D = 0 \quad (15) \end{aligned}$$

with

$$A = -2\alpha^4 \quad (16)$$

$$B = \alpha^2 (h_c - h_w) \quad (17)$$

$$C = 2\alpha^2 (T_w h_w + T_c h_c) \quad (18)$$

$$D = 2h_w h_c (T_c - T_w) \quad (19)$$

Although Eq. (15) is rather complicated, a numeric solution for  $\Delta T_{teg}$  can be calculated when the heat exchanger and TEG parameters are known. Once the temperature difference across the TEG is known, the electrical power output is determined from the product of the current squared and the load resistance.

$$P = \left( \frac{\alpha \Delta T_{teg}}{R_t} \right)^2 R_l \quad (20)$$

FIXED JUNCTION TEMPERATURE DESIGN PERFORMANCE - The design of TEGs often neglects the temperature drop

across the heat exchanger surface. For many higher temperature applications this assumption is reasonable. However, the temperature drop across the heat exchanger is determined by the TEG design, and illustration of this interaction is informative.

For convenience, Eq. (15), which describes the TEG and heat exchanger interaction, is modified to express the TEG design by:

$$n = R_g/R \quad (21)$$

$$m = \gamma_n/\gamma_p \quad (22)$$

$$\gamma = \gamma_p \text{ COV} \quad (23)$$

These expressions and Eqs. (5) and (7), are used to replace  $R_g$ ,  $R$ , and  $K$ . Defining

$$Z = \frac{\Delta T_{\text{teg}}}{R_c} \quad (24)$$

the resulting polynomial is

$$\begin{aligned} nAZ^3 + B(2n+1)Z^2 \\ + \left[ 2\alpha(n+1)(h_w+h_c) + 2\alpha(n+1)(h_w+h_c)(m\lambda_n+\lambda_p) \right. \\ \left. + \frac{\gamma C}{\rho_n/m + \rho_p} \right] Z + \frac{\gamma D}{\rho_n/m + \rho_p} = 0 \end{aligned} \quad (25)$$

The power output of a heat exchanger-TEG system is affected by numerous parameters. Since this paper has evolved from investigating TEG performance in an OTEC application, heat transfer coefficients and flow temperatures representative of OTEC systems are considered. Also, the values of the  $p$  and  $n$  materials approach current limits of technology. These parameter values are given in Table 1.

Table 1 - Constants for OTEC Heat Exchanger-TEG Example

Flow temperatures

$$T_w = 25^\circ\text{C}$$

$$T_c = 5^\circ\text{C}$$

Heat Transfer Coefficients

$$h_w = 0.5 \text{ W/cm}^2 \text{ }^\circ\text{C}$$

$$h_c = 0.3 \text{ W/cm}^2 \text{ }^\circ\text{C}$$

Thermoelectric Properties

n-type material

p-type material

$$\alpha = 0.143 \times 10^{-3} \text{ V/}^\circ\text{C}$$

$$0.173 \times 10^{-3} \text{ V/}^\circ\text{C}$$

$$\rho = 0.79 \times 10^{-3} \text{ } \Omega \text{ cm}$$

$$0.87 \times 10^{-3} \text{ } \Omega \text{ cm}$$

$$\lambda = 8.1 \times 10^{-3} \text{ W/cm }^\circ\text{C}$$

$$8.7 \times 10^{-3} \text{ W/cm }^\circ\text{C}$$

Figure of merit  $3.2 \times 10^{-3} \text{ K}^{-1}$   $3.4 \times 10^{-3} \text{ K}^{-1}$

Now only the design parameters  $\gamma$ ,  $n$ , and  $m$  need to be investigated. Two standard fixed junction temperature design methods are examined: maximum efficiency and maximum power constraints. They are:

for maximum efficiency

$$m = \left( \frac{\rho_n \lambda_p}{\rho_p \lambda_n} \right)^{1/2} \quad (26)$$

$$n = \left[ 1 + \left( \frac{\alpha}{\sqrt{\frac{\rho_n \lambda_n}{\rho_p \lambda_p}} + \sqrt{\frac{\rho_p \lambda_p}{\rho_n \lambda_n}}} \right)^2 \left( \frac{T_{wj} + T_{cj}}{2} \right) \right]^{1/2} \quad (27)$$

and for maximum power

$$m = \left( \frac{\rho_n}{\rho_p} \right)^{1/2} \quad (28)$$

$$n = 1 \quad (29)$$

Since no constraint is applied to  $\gamma$ , performance of the heat exchanger-TEG system is evaluated for a wide range of  $\gamma$ . Results are illustrated in Figs. 2 and 3.

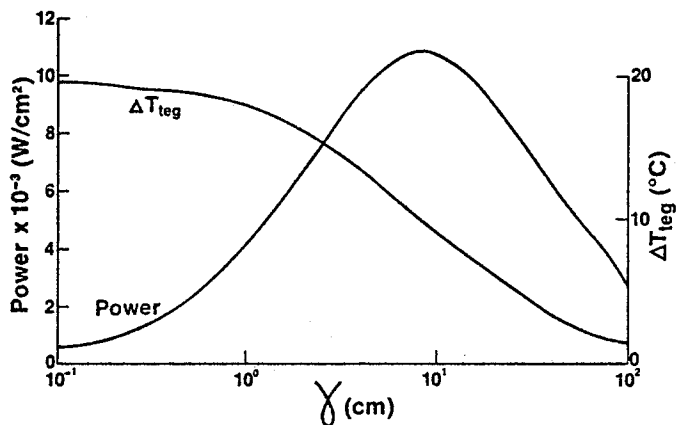


Fig. 2 - Heat exchanger-TEG performance using fixed-junction-temperature maximum-efficiency constraints

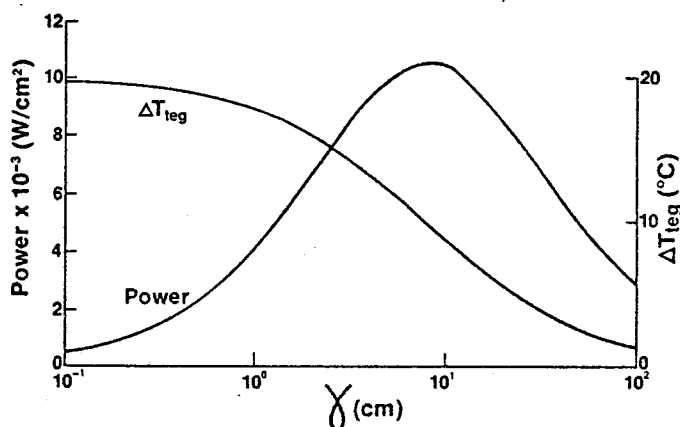


Fig. 3 - Heat exchanger-TEG performance using fixed-junction-temperature maximum-power constraints

Inspection of Figs. 2 and 3 shows little variation in performance between maximum-efficiency and maximum-power fixed-junction-temperature constraints. However, for this calculation the largest value of electrical output power occurs when maximum efficiency, not maximum power, constraints are used. This

is an obvious error and illustrates one limitation of applying fixed temperature analysis on heat exchanger-TEG systems with significant temperature drops across the heat exchanger surfaces. Also, fixed junction temperature techniques do not address the important relationship between  $\gamma$  and  $\Delta T_{\text{teg}}$ . In practice, an acceptable value for  $\gamma$  that results in a satisfactory trade-off between heat exchanger losses and reduced conversion efficiency may be found by trial and error.

**MAXIMUM POWER CONDITIONS** - To design a TEG imbedded within a heat exchanger that will deliver maximum power, appropriate values of  $\gamma$ ,  $n$ , and  $m$  need to be identified. The method of Lagrange multipliers is well-suited to this optimization problem. The problem restated is to maximize the power function

$$P = \alpha^2 Z^2 R_2 \quad (30)$$

subject to the constraints that describe the heat exchanger-TEG system.

An analytic solution for  $m$  can be readily found by using Eqs. (5), (7), and (15) as constraints on the power function. These equations are restated in terms of  $\gamma$ ,  $m$ ,  $R$ ,  $R_2$ ,  $K$ , and  $Z$ .

$$F_1(\gamma, m, K) = (\lambda_n + \lambda_p) \gamma - K = 0 \quad (31)$$

$$F_2(\gamma, m, R) = \left( \frac{\rho_n}{m} + \rho_p \right) / \gamma - R = 0 \quad (32)$$

$$F_3(Z, K, R, R_2) = R_2 \alpha Z^3 + B(2R_2 + R)Z^2 + [2(R + R_2)(h_w h_c + h_w K + h_c K) + C]Z + D = 0 \quad (33)$$

The maximum occurs when

$$\begin{aligned} \nabla P(Z, R_2) - L_1 \nabla F_1(\gamma, m, K) - L_2 \nabla F_2(\gamma, m, R) \\ - L_3 \nabla F_3(Z, R_2, K, R) = 0 \end{aligned} \quad (34)$$

Looking only at the partial derivatives of Eq. (34) with respect to  $m$  and  $\gamma$  yields

$$-L_1 \lambda_n \gamma + \frac{L_2 \rho_n}{\gamma m^2} = 0 \quad (35)$$

$$L_1 (\lambda_n + \lambda_p) + L_2 \left( \frac{\rho_n}{m} + \rho_p \right) / \gamma^2 = 0 \quad (36)$$

These two equations may be equated to yield

$$m = \left( \frac{\rho_n \lambda_p}{\rho_p \lambda_n} \right)^{1/2} \quad (37)$$

With the constraint on  $m$  satisfying the maximum power condition, a single constraint,  $G(Z, n, \gamma)$ , on the power function is developed from Eq. (25):

$$G(Z, n, \gamma) = n \alpha Z^3 + B(2n + 1)Z^2 + [(n + 1)(2h_w h_c + \gamma E) + \frac{\gamma C}{F}]Z + \gamma \frac{D}{F} = 0 \quad (38)$$

with the additional constants.

$$E = 2(h_w + h_c)(m \lambda_n + \lambda_p) \quad (39)$$

$$F = \frac{\rho_n}{m} + \rho_p \quad (40)$$

Eq. (38), the constraint on the power function, is dependent on  $\gamma$ ,  $n$ , and  $Z$ . Power expressed in these variables is

$$P = \frac{\alpha^2 Z^2 n F}{\gamma} \quad (41)$$

Again, the maximum power condition must satisfy the Lagrange multiplier expression

$$\nabla P(Z, n, \gamma) - L_1 \nabla G(Z, n, \gamma) = 0 \quad (42)$$

This gradient expression and Eq. (38) yield the four nonlinear simultaneous equations:

$$\begin{aligned} h_1(Z, n, \gamma, L) = \frac{2 \alpha^2 n F Z}{\gamma} - L_1 [3 \alpha n Z^2 + 2B(2n+1)Z \\ + 2n h_w h_c + n \gamma E + \gamma(E + \frac{C}{F}) + 2h_w h_c] \\ = 0 \end{aligned} \quad (43)$$

$$h_2(Z, n, \gamma, L_1) = \frac{\alpha^2 F Z}{\gamma} - L_1 (\alpha Z^2 + 2BZ + 2h_w h_c + \gamma E) = 0 \quad (44)$$

$$h_3(Z, n, \gamma, L_1) = \frac{\alpha^2 F Z^2 n}{\gamma^2} + L_1 \left[ (nE + E + \frac{C}{F})Z + \frac{D}{F} \right] = 0 \quad (45)$$

$$h_4(Z, n, \gamma, L_1) = G(Z, n, \gamma) \quad (46)$$

These expressions provide sufficient information to determine the values of  $Z$ ,  $n$ ,  $\gamma$ , and  $L_1$  that satisfy the maximum power condition. However, solution of these four nonlinear equations is extremely difficult analytically. Consequently, a numeric iterative approach is better suited.

Newton's method has been used successfully. When an approximate solution of  $Z$ ,  $n$ ,  $\gamma$ , and  $L_1$  is known, an improved estimate is found by adding a correction to the current approximate solution. With

$$\begin{bmatrix} Z \\ n \\ \gamma \\ L_1 \end{bmatrix} = \bar{x} \quad (47)$$

and

$$[H] \bar{x} = [h_1(\bar{x}), h_2(\bar{x}), h_3(\bar{x}), h_4(\bar{x})]^T \quad (48)$$

the correction  $\bar{y}$  satisfies the linear simultaneous equations:

$$[H]' \bar{y} = [H] \bar{x} \quad (49)$$

In Eq. (49),  $[H]'$  is the Jacobian matrix of  $[H]$  (3).

Using the constraints applied previously on the heat exchanger, flow temperatures, and thermoelectric material, the maximum power solution has been calculated and is presented in Table 2.

**APPROXIMATE MAXIMUM POWER MODEL** - Analysis of several heat exchanger-TEG systems has shown that maximum power generation occurs when  $\Delta T_{\text{teg}}$  is approximately

Table 2 - Maximum Power Operating Conditions for the Heat Exchanger-TEG Example

$T_{wj}$ = 21.24°C	$T_{cj}$ = 11.23°C
$\gamma$ = 8.294 cm <sup>2</sup> /cm	$n$ = 1.399
Power = 1.078 x 10 <sup>-2</sup> W/cm <sup>2</sup>	$\eta$ = 0.57367%

equal to one-half of the total available temperature difference between the warm and cold flows and maximum efficiency fixed temperature constraints are applied to the TEG. This result, which is almost intuitively obvious, yields a quite simple approximate approach for designing a TEG to yield maximum power.

With  $\eta$ , the conversion efficiency, the TEG power output can be calculated from the heat flux passing through the warm side of the heat exchanger

$$P = \Delta T_w h_w \eta \quad (50)$$

Applying conservation of energy through the TEG, the warm and cold heat fluxes are related by

$$\Delta T_w h_w = \Delta T_c h_c + \Delta T_w h_w \eta \quad (51)$$

This approximate maximum power solution uses the assumptions that

$$\Delta T_{teg} = \frac{(T_w + T_c)}{2} \quad (52)$$

The additional assumption is that the TEG is designed to maximize efficiency at its operating temperature. Applying this constraint, the ratio of the load resistance to internal resistance is calculated from Eq. (27). The resulting conversion efficiency is known to be

$$\eta = \frac{(n-1) \Delta T_{teg} / T_{wj}}{(n+T_{wj}/T_{cj})} \quad (53)$$

which is the maximum efficiency possible for a TEG operating under fixed junction temperatures (2).

Using Eqs. (10), (51), and (52) the resulting expression for the temperature drop across the warm flow heat exchange surface is

$$\Delta T_w = \frac{h_c \Delta T_{teg}}{h_w (1-\eta) + h_c} \quad (54)$$

In Eqs. (27) and (53), the junction temperatures are assumed to be known. This is not the case, but the solution can be rapidly found by iterating through Eqs. (27), (53), and (54) several times. The convergence progresses by setting the junction temperatures at  $T_w$  and  $T_c$  and then refining their estimates after  $\Delta T_w$  has been calculated. Accurate values for  $n$ ,  $\eta$ , and  $\Delta T_w$  are obtained in three or so iterations. After this convergence is completed, the necessary value of  $\gamma$  is calculated from

$$\gamma = \frac{h_w F \Delta T_w \eta (n+1)^2}{\alpha^2 \Delta T_{teg}^2 n} \quad (55)$$

This expression for  $\gamma$  is found by equating the power expressions (41) and (50) and replacing  $Z$  by

$$Z = \frac{\Delta T_{teg} \gamma}{F(n+1)} \quad (56)$$

Using this approximate design technique on the previously used example system yields results similar to the actual maximum power solution developed previously. These results are tabulated in Table 3. The operating point varies slightly, but power generation is reduced by only 0.0001%. Agreement is well within experimental tolerances, and little if any improvement is possible by using the exact maximum power solution.

Table 3 - Comparison of Actual and Approximate Maximum Power Solutions

Actual Maximum Power		Approximate Maximum Power	
$P$	= 10.78 X 10 <sup>-3</sup> W/cm <sup>2</sup>	$P$	= 10.78 X 10 <sup>-3</sup> W/cm <sup>2</sup>
$\gamma$	= 8.29 cm	$\gamma$	= 8.31
$n$	= 1.40	$n$	= 1.40
$\Delta T_{teg}$	= 10.01°C	$\Delta T_{teg}$	= 10.00°C

ADDITIONAL HEAT EXCHANGER COMMENTS - The preceding discussion considers TEG design when the heat transfer coefficients of the heat exchanger surfaces are known. To actually design a TEG for maximum power generation, the additional system losses need to be subtracted from the TEG output power. The major loss in an OTEC application is the pumping power.

For heat exchangers, the heat transfer coefficient increases roughly linearly with Reynolds number, while pumping losses are more closely related to the cube of the Reynolds number. Figure 4 illustrates a typical relationship between gross TEG power and net system power for a range of Reynolds numbers. As is obvious from the graph, the net power generation of a heat exchanger-TEG system achieves a maximum at a specific Reynolds number.

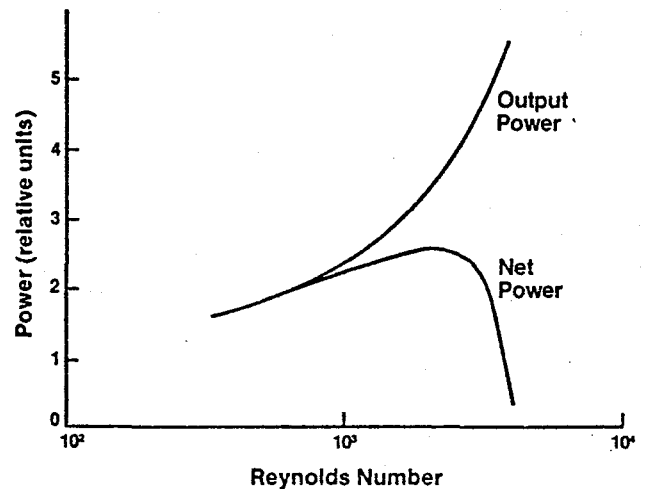


Fig. 4 - TEG power output and heat exchanger-TEG system power output

Normally the Reynolds number for the warm and cold flows will differ at the point of maximum power generation. Since heat exchanger analysis is not well suited to analytic description, numeric trial and error of various Reynolds numbers for the warm and cold flows is a direct method for locating a desirable operating point.

#### CONCLUSION

Conventional fixed temperature TEG analysis techniques are inadequate for investigating heat exchanger-TEG system performance. Analysis of such sys-

tems illustrates the relationship between the thermoelectric element area-to-length ratio and both the available temperature difference across the TEG and the resulting electric power generation. For applications, such as OTEC, where maximum power generation is desired, detailed and simplified numeric techniques for designing TEGs within heat exchanger-TEG systems are presented.

#### REFERENCES

1. T. S. Jayadev, et al., "Thermoelectric OTEC," 6th OTEC Conference, Washington, D.C., June 1979.
2. S. W. Angrist, "Direct Energy Conversion," Boston, Allyn and Bacon, Inc., 1971.
3. J. M. Ortega, "Numerical Analysis: A Second Course," New York, Academic Press., 1972.